

1 **Reduced Antarctic meridional overturning circulation reaches the**  
2 **North Atlantic Ocean**

3  
4 Gregory C. Johnson<sup>1,2</sup>, Sarah G. Purkey<sup>1,2</sup>, and John M. Toole<sup>3</sup>

5  
6 <sup>1</sup>Pacific Marine Environmental Laboratory, NOAA

7 Seattle, Washington, USA

8  
9 <sup>2</sup>School of Oceanography, University of Washington

10 Seattle, Washington, USA

11  
12 <sup>3</sup>Department of Physical Oceanography, Woods Hole Oceanographic Institution

13 Woods Hole, Massachusetts, USA

14  
15 for *Geophysical Research Letters*

16 Submitted 7 August 2008

17

18

18           **Abstract.** We analyze abyssal temperature data in the western North Atlantic  
19 Ocean from the 1980's – 2000's, showing that reductions in Antarctic Bottom Water  
20 (AABW) signatures have reached even that basin. Trans-basin oceanographic sections  
21 occupied along 52°W from 1983 – 2003 and 66°W from 1985 – 2003 quantify abyssal  
22 warming resulting from deepening of the strong thermal boundary between AABW and  
23 North Atlantic Deep Water (NADW), hence a local AABW volume reduction. Repeat  
24 section data taken from 1981 – 2004 along 24°N also show a reduced zonal gradient in  
25 abyssal temperatures, consistent with decreased northward transport of AABW. The  
26 reduction in the Antarctic limb of the MOC within the North Atlantic highlights the  
27 global reach of climate variability originating around Antarctica.

28

29           **Index Terms.** 1635 Global Change: Oceans; 4207 Arctic and Antarctic oceanography,  
30 4283 Water masses, 4513 Decadal ocean variability, 4532 General circulation

31

32           **Keywords:** Antarctic Bottom Water, Meridional Overturning Circulation

33

34

## 34 1. Introduction

35 The deep ocean is important to Earth's climate, storing substantial  
36 anthropogenic heat [Levitus *et al.*, 2006], contributing to sea level rise [Domingues *et*  
37 *al.*, 2008], and globally transporting heat, freshwater, and biogeochemical parameters.  
38 Shutdown of the North Atlantic Deep Water (NADW) sinking limb of the Meridional  
39 Overturning Circulation (MOC) is a proposed initiator of past rapid climate change  
40 [Broecker, 1998]. However, the other MOC limb, fed by sinking Antarctic Bottom  
41 Water (AABW), is of comparable size [Orsi *et al.*, 1999] with AABW covering about  
42 twice as much ocean floor as NADW and occupying about twice its volume [Johnson,  
43 2008].

44 As it spreads northward into each of the three major oceans, AABW mixes with  
45 overlying waters, but nevertheless, AABW influences can be traced even to the western  
46 basins of the North Atlantic [Orsi *et al.*, 1999; Johnson, 2008]. AABW has warmed  
47 around the globe over the past few decades. Weddell Sea Bottom Water, the coldest,  
48 densest variety of AABW, warmed and lost volume during the 1990's [Fahrbach *et al.*,  
49 2004]. From the 1970's through the 1990's Warm Deep Water, another AABW  
50 constituent, also warmed by  $\sim 0.01$  °C yr<sup>-1</sup> in the Ross [Jacobs *et al.*, 2002] and Weddell  
51 [Robertson *et al.*, 2002] Seas. Downstream of the AABW formation regions,  
52 comparisons of potential temperature ( $\theta$ ) data collected on sections repeated one or  
53 more times since the 1980's reveal abyssal warming in deep basins ventilated by  
54 AABW in the Southeast Indian [Johnson *et al.*, 2008], Pacific [Fukasawa *et al.*, 2003;  
55 Kawano *et al.*, 2006; Johnson *et al.*, 2007], western South Atlantic [Coles *et al.*, 1996;  
56 Johnson and Doney, 2006; Zenk and Morozov, 2007], and even equatorial Atlantic  
57 [Hall *et al.*, 1997; Andrié *et al.*, 2003], Oceans although in the last not unambiguously

58 [Limeburner *et al.*, 2005]. In addition, the strong vertical  $\theta$  gradient (the deep  
59 thermocline) between NADW and AABW deepened in the South Atlantic and on the  
60 equator [Johnson and Doney, 2006; Limeburner *et al.*, 2005]. A reduction of AABW  
61 influence, communicated not by advection but by Kelvin and Rossby Waves in the  
62 presence of local lateral and vertical gradients, could produce such warming on these  
63 time scales [Nakano and Suginozono, 2002].

64 Here ten data sets from three sections repeatedly occupied in the western North  
65 Atlantic (Figure 1) are analyzed with respect to AABW changes. Two repeated  
66 meridional sections [Joyce *et al.*, 1999], one along 52°W (occupied in 1981, 1997, and  
67 2003) and the other along 66°W (occupied in 1985, 1997, and 2003), both reveal  
68 AABW warming. In addition, a repeated zonal section [Bryden *et al.*, 2005; Longworth,  
69 2007] along 24°N (occupied in 1981, 1992, 1998, and 2004) shows a reduction in  
70 northward AABW transport.

71

## 72 **2. Data and Analysis Methods**

73 For this study modern post-1980 oceanographic data from repeat sections along  
74 52°W, 66°W, and 24°N are analyzed to assess time variability of abyssal ocean  $\theta$ , its  
75 statistical significance, and geostrophic volume transport variability. The 1980's  
76 sections were occupied during the ramp-up to the World Ocean Circulation Experiment  
77 (WOCE). The 1990's sections were occupied during WOCE. The 2000's sections were  
78 occupied in support of CLIVAR (Climate Variability) and Carbon Cycle Science  
79 Programs.

80 Vertical profiles of specific volume anomaly and  $\theta$  on the 1968 International  
81 Practical Temperature Scale are calculated from the data at each station. The quantities

82 are then interpolated onto a closely spaced pressure-latitude (or pressure-longitude) grid  
83 and masked using bottom bathymetry before differences, means, or velocities are  
84 calculated. Degrees of freedom for the differences are estimated from integrals of their  
85 spatially lagged autocorrelations [von Storch and Zwiers, 2001] at each pressure.  
86 Student's T-test is then applied to estimate the 95% confidence intervals.

87         The data from these sections are especially useful for detecting subtle changes in  
88 abyssal temperatures for three reasons. Firstly, these sections all have stations that are  
89 relatively closely spaced in the horizontal, generally having nominal distances of 55 km  
90 between stations. Secondly, these sections all employ a CTD (Conductivity-  
91 Temperature-Depth) instrument, which allows very accurate ( $\pm 0.002$  °C) temperature  
92 measurements [Joyce *et al.*, 1999]. Thirdly, the CTD data are vertically continuous, and  
93 located in the vertical by very accurate ( $\pm 2$  dbar) pressure measurements from the sea  
94 surface to the ocean floor.

95         To ensure comparison of only geographically co-located data, at each longitude  
96 (or latitude) of the grid, only data shallower than the shallowest of a set of straight lines  
97 (one for each section) connecting the deepest sample pressures of adjacent stations  
98 versus longitude (or latitude) are used in the analysis. In addition to this mask, data at  
99 grid points exceeding the pressure corresponding to a bathymetric estimate [Smith and  
100 Sandwell, 1997] for each grid location are also discarded. Small deviations in  
101 individual section longitudes from  $52^\circ\text{W}$  and  $66^\circ\text{W}$  and latitudes from  $24^\circ\text{N}$  (Figure 1)  
102 are ignored. However, calculations of  $\theta$  differences and geostrophic velocities are  
103 generally limited to regions where deviations from the nominal section longitude (or  
104 latitude) are small.

105

### 106 3. Results

107 Consistent with climatological [*Gouretski and Koltermann, 2004*] bottom  $\theta$  in  
108 the western North Atlantic (Figure 1), the strongest AABW influence along the  $52^\circ\text{W}$   
109 section is at its southern end, from  $8 - 18^\circ\text{N}$ , and below 4500 dbar (Figure 2a). There  
110 the strong abyssal thermocline from 4500 – 5000 dbar marks the vertical transition  
111 between NADW and AABW. Only from  $8 - 18^\circ\text{N}$  do the time-mean near-bottom  $\theta$ s  
112 drop below  $1.5^\circ\text{C}$ , indicating strong AABW influence. To the north, where the AABW  
113 influence is diminished, near-bottom  $\theta$ s are much higher.

114 Subtracting gridded 1983  $\theta$ s from 2003 values at each location (Figure 2a)  
115 quantifies warming exceeding  $0.1^\circ\text{C}$  on average from  $8 - 18^\circ\text{N}$  near 4900 dbar (Figure  
116 2b). The abyssal warming, significantly different from zero at 95% confidence from  
117 3800 – 5000 dbar, is caused by 80 – 150 dbar sinking of the abyssal thermocline in this  
118 region. The deep 1997 – 1983 section-mean differences from  $8 - 18^\circ\text{N}$  lie between the  
119 2003 – 1983 values, consistent with monotonic warming.

120 Along  $66^\circ\text{W}$ , AABW influence is evident from about  $18 - 27^\circ\text{N}$  (Figure 3a),  
121 where bottom  $\theta$ s are coldest, and the abyssal thermocline strongest. However,  
122 everywhere along  $66^\circ\text{W}$  the time-mean near-bottom  $\theta$ s exceed  $1.4^\circ\text{C}$ , warmer than  
123 values seen along  $52^\circ\text{W}$ , as in climatological bottom  $\theta$  (Figure 1). The abyssal  
124 thermocline at  $66^\circ\text{W}$ , located from 5000 – 5550 dbar, is weaker than at  $52^\circ\text{W}$ , and is  
125 also deeper by  $\sim 500$  dbar. Unlike at  $52^\circ\text{W}$ , a relatively homogenous bottom layer in  $\theta$ ,  
126  $\sim 500$ -dbar thick, fills the southern end of the basin at  $66^\circ\text{W}$ . These features are  
127 signatures of an AABW layer cascading downward and northwestward along the  
128 deepening seafloor from the equator into the western North Atlantic.

129 As at 52°W, subtracting 1985  $\theta$ s from 2003 values along 66°W shows warming  
130 within the abyssal thermocline and the nearly homogenous bottom layer below (Figure  
131 3a). This warming is strongest south of 22°N around 5200 dbar. The warming within  
132 the AABW-influenced waters for 2003 – 1985 is  $\sim 0.02$  °C from 18 – 27°N (Figure 3b).  
133 Within the abyssal thermocline, warming occurred prior to 1997 while bottom layer  
134 warming is post 1997 and significant at 95%.

135 The 24°N section data reveal a classic signature of northward flowing AABW  
136 [*Wright, 1970*]. A strong zonal gradient in  $\theta$  is present for  $P > 4000$  dbar ( $\theta < 2.0$  °C),  
137 with potential isotherms overall rising to the east over the western flank of the mid-  
138 ocean ridge (Figure 4a). With an interior mid-depth zero-velocity surface, application  
139 of the geostrophic relation to the mean density structure yields increasingly northward  
140 flow toward the bottom below these sloping isotherms. In contrast, near the western  
141 boundary, isotherms rise westward, a signature of the southward-flowing deep-western  
142 boundary-current of NADW below  $\sim 1000$  dbar [*Bryden et al., 2005*]. Also, isotherms  
143 plunge downward toward the ridge within  $\sim 1000$  dbar of the bottom, likely the result of  
144 mixing over the complex ridge topography [*Mauritzen et al., 2002*].

145 Subtracting 1981  $\theta$ s from 2004 values at 24°N reveals a basin-scale pattern  
146 (Figure 4a). Warming is evident east of  $\sim 57^\circ\text{W}$ , and cooling west of that longitude.  
147 This pattern is caused by isotherms deepening east of 57°W, and shoaling to the west. It  
148 is consistent with a reduced net northward volume transport of AABW in 2004 versus  
149 1981. To quantify this reduction, data from four sections occupied along 24°N are used  
150 to calculate geostrophic meridional velocities employing a 3200-dbar zero-velocity  
151 surface [*Bryden et al., 2005*]. Volume transport integrations are limited to the western  
152 basin interior (70 – 46°W) to exclude the deep-western boundary-current, and to water

153 with  $\theta < 1.8$  °C to isolate the AABW [Bryden *et al.*, 2005]. Northward volume  
154 transport of AABW estimated from the sections across 24°N decreases monotonically  
155 from 1981 – 2004 (Figure 4b).

156

#### 157 **4. Discussion**

158 The finding of a northward transport reduction of AABW at 24°N merits some  
159 caveats. Data from an instrument array monitoring the Atlantic MOC reveals transport  
160 variations exceeding 30% during a single year [Cunningham *et al.*, 2007], suggesting a  
161 decadal 30% MOC reduction inferred from analysis of trans-Atlantic sections occupied  
162 along 24°N [Bryden *et al.*, 2005] could be aliased short timescale variability. In  
163 addition, although previously employed [Bryden *et al.* 2005], the 3200-dbar zero-  
164 velocity surface is overly simplistic. The circulation in the deep-western boundary-  
165 current (while excluded here) is also complex and strongly time-dependent  
166 [Cunningham *et al.*, 2007]. Nonetheless, the large-scale changes observed at 24°N are  
167 consistent with a monotonic reduction in the large-scale northward flow of AABW there  
168 from 1981 – 2004.

169 A  $4 \times 10^6$  m<sup>3</sup> s<sup>-1</sup> reduction in northward transport of AABW into the North  
170 Atlantic applied steadily over 23 years yields a volume reduction of  $1.5 \times 10^{15}$  m<sup>3</sup>. The  
171 climatological [Gouretski and Koltermann, 2004] volume of water in the western basins  
172 of the North Atlantic from 0 – 48°N with  $\theta < 1.8$  °C is  $4.0 \times 10^{15}$  m<sup>3</sup>, with average  
173 thickness of 690 m over an area of  $5.8 \times 10^{12}$  m<sup>2</sup>. Thus the inferred volume reduction of  
174 AABW is 37% of its climatological value, grossly consistent with the warming reported  
175 here originating from some combination of isotherm deepening and lateral retraction  
176 within the AABW.



177           This analysis reveals various signatures of AABW retreat in the western basins  
178 of the North Atlantic. At the southern ends of both the 52°W and 66°W sections, the  
179 abyssal thermocline between NADW and AABW deepens from the early 1980's to  
180 2003. This deepening results in a reduction of AABW volume there. In addition, the  
181 500-m thick layer of AABW found below that thermocline at 66°W exhibits a warming  
182 of ~0.02 °C from 1997 to 2003, significant at 95%, another signature of reduced AABW  
183 influence. At both longitudes, the 1997 values are mostly intermediate between those of  
184 the earlier and later sections. Finally, estimated northward volume transports of AABW  
185 across 24°N decrease with time as the result of a large-scale reduction in the zonal  
186 temperature gradient across the deep portions of the western basin. In addition, the  
187 AABW warming or volume reductions over the past few decades reported in so many  
188 different data sets and so many analyses to the south, from its Southern Ocean origins to  
189 the equatorial Atlantic, as detailed in the introduction, support the analyses presented  
190 here for the North Atlantic.

191           AABW warming reduces its density [*Jacobs et al.*, 2002], and perhaps its  
192 formation rate. The AABW warming may be as geographically widespread as AABW  
193 itself, which covers much of the global ocean floor and often extends over 1000's of  
194 meters in the vertical [*Johnson*, 2008]. Thus, AABW warming over the past decade  
195 should contribute to global heat and sea level budgets, helping to close recent reported  
196 multi-decadal [*Domingues et al.*, 2008], and perhaps interannual [*Willis et al.*, 2008]  
197 imbalances among sea level, mass, and upper ocean heat budgets.

198

199           **Acknowledgments.** NOAA and NSF supported the 2003 U.S. CLIVAR/CO<sub>2</sub>  
200 Repeat Hydrography Program reoccupations of the 52°W and 66°W sections, led by

201 Chief Scientists Drs. John Toole and Terrence Joyce, respectively. The U. K. National  
202 Environment Research Council supported the 2004 reoccupation of the 24°N section,  
203 led by Chief Scientist Dr. Stuart Cunningham. The hard work of all contributing to the  
204 collection and processing of data analyzed here is gratefully acknowledged. The  
205 NOAA Office of Oceanic and Atmospheric Research and the NOAA Climate Program  
206 Office supported the analysis. Findings and conclusions in this article are those of the  
207 authors and do not necessarily represent the views of NOAA. PMEL Contribution  
208 Number 3227.

209

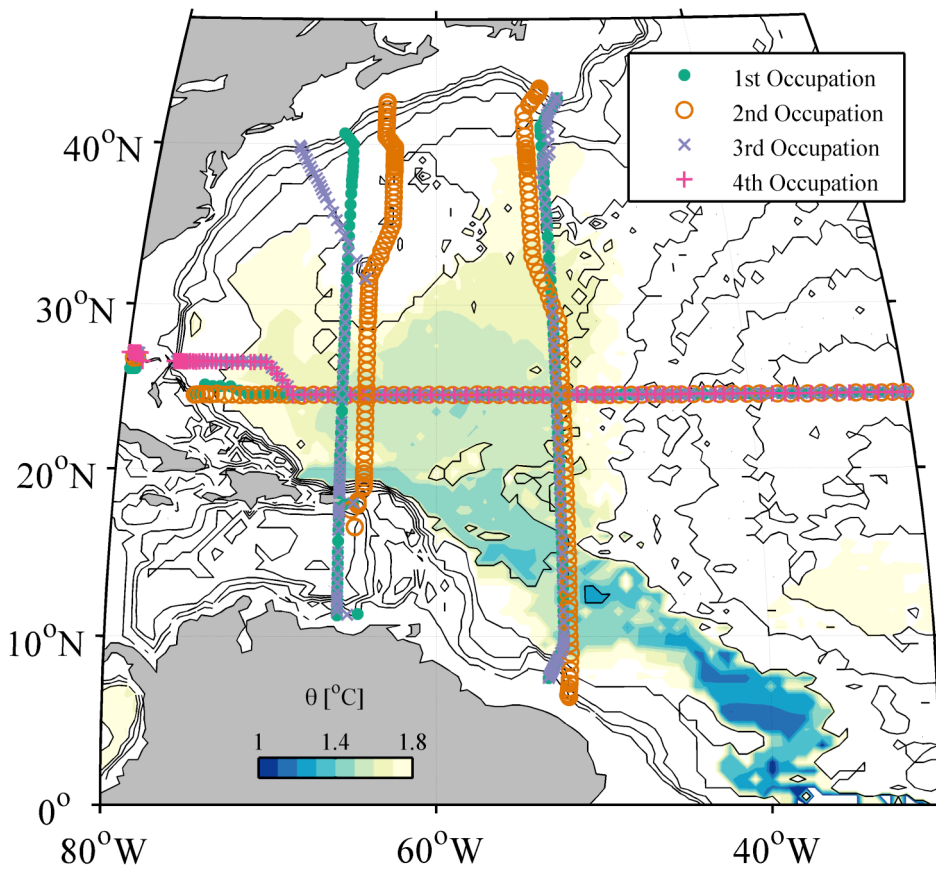
## 210 **References**

- 211 Andrié, C., Y. Gouriou, B. Bourlès, J.-F. Ternon, E. S. Braga, P. Morin, and C. Oudot  
212 (2003), Variability of AABW properties in the equatorial channel at 35°W,  
213 *Geophys. Res. Lett.*, *30*, 8007, doi:10.1029/2002GJ015766.
- 214 Broecker, W. S. (1998), Paleocean circulation during the last deglaciation: A bipolar  
215 seasaw? *Paleoceanogr.*, *13*, 119–121.
- 216 Bryden, H. L., H. R. Longworth, and S. A. Cunningham (2005), Slowing of the Atlantic  
217 meridional overturning circulation at 24°N, *Nature*, *438*, 655–657.
- 218 Coles, V. J., M. S. McCartney, D. B. Olson, and W. M. Smethie Jr. (1996), Changes in  
219 Antarctic Bottom Water properties in the western South Atlantic in the late 1980s, *J.*  
220 *Geophys. Res.*, *101*, 8957–8970.
- 221 Cunningham, S. A., T. Kanzow, D. Rayner, M. O. Baringer, W. E. Johns, J. Marotzke,  
222 H. R. Longworth, E. M. Grant, J.J.-M. Hirschi, L. M. Beal, C. S. Meinen, and H. L.  
223 Bryden (2007), Temporal variability of the Atlantic meridional overturning  
224 circulation at 26.5°N, *Science*, *317*, 935–938.

- 225 Domingues, C. M., J. A. Church, N. J. White, P. J. Gleckler, S. E. Wijffels, P. M.  
226 Barker, and J. R. Dunn (2008), Improved estimates of upper ocean warming and  
227 multi-decadal sea level rise, *Nature*, *453*, 1090–1093.
- 228 Fahrbach, E., M. Hoppema, G. Rohardt, M. Schröder, and A. Wisotzki (2004), Decadal-  
229 scale variations of water mass properties in the deep Weddell Sea, *Ocean Dynamics*,  
230 *54*, 77–91.
- 231 Fukasawa, M., H. Freeland, R. Perkin, T. Watanabe, H. Uchida, and A. Nishima (2004),  
232 Bottom water warming in the North Pacific Ocean, *Nature*, *427*, 825–827.
- 233 Gouretski, V. V. and K. P. Koltermann (2004), *WOCE Global Hydrographic*  
234 *Climatology*, Berichte des Bundesamtes für Seeschifffahrt und Hydrographie, *35*,  
235 pp. 52 + 2 CD-ROMs.
- 236 Hall, M. M., M. S. McCartney, and J. A. Whitehead (1997), Antarctic Bottom Water  
237 flux in the equatorial western Atlantic, *J. Phys. Oceanogr.*, *27*, 1903–1926.
- 238 Jacobs, S. S., C. F. Giulivi, and P. A. Mele (2002), Freshening of the Ross Sea during  
239 the late 20<sup>th</sup> century, *Science*, *297*, 386–389.
- 240 Johnson, G. C. (2008), Quantifying Antarctic Bottom Water and North Atlantic Deep  
241 Water volumes. *J. Geophys. Res.*, *113*, C05027, doi:10.1029/2007JC004477.
- 242 Johnson, G. C. and S. C. Doney (2006), Recent western South Atlantic bottom water  
243 warming, *Geophys. Res. Lett.*, *33*, L14614, doi:10.1029/2006GL026769.
- 244 Johnson, G. C., S. Mecking, B. M. Sloyan, and S. E. Wijffels (2007), Recent bottom  
245 water warming in the Pacific Ocean, *J. Climate*, *20*, 5365–5375.
- 246 Johnson, G. C., S. G. Purkey, and J. L. Bullister, (2008) Warming and freshening in the  
247 abyssal southeastern Indian Ocean, *J. Climate*, in press,  
248 doi:10.1175/2008JCLI2384.1.

- 249 Joyce, T. M., R. S. Pickart, and R. C. Millard (1999), Long-term hydrographic changes  
250 at 52 and 66°W in the North Atlantic Subtropical Gyre & Caribbean, *Deep-Sea Res.*  
251 *II*, 46, 245–278.
- 252 Kawano, T., M. Fukawasa, S. Kouketsu, H. Uchida, T. Doi, I. Kaneko, M. Aoyama, and  
253 W. Scheider (2006), Bottom water warming along the pathways of lower  
254 circumpolar deep water in the Pacific Ocean, *Geophys. Res. Lett.*, 33, L23613,  
255 doi:10.1029/2006GL027933.
- 256 Levitus, S., J. Antonov, and T. Boyer (2005), Warming of the world ocean, 1955–2003,  
257 *Geophys. Res. Lett.*, 32, L02604, doi:10.1029/2004GL021592.
- 258 Limeburner, R., J. A. Whitehead, and C. Cenedese (2005), Variability of Antarctic  
259 Bottom Water flow into the North Atlantic, *Deep-Sea Res. II*, 52, 495–512.
- 260 Longworth, H. R. (2007), Constraining variability of the Atlantic Meridional  
261 Overturning Circulation at 25°N from historical observations, 1980 to 2005, Ph. D.  
262 Thesis, 197 pp., University of Southampton.
- 263 Mauritzen, C., K. L., Polzin, M. S. McCartney, R. C. Millard, and D. E. West-Mack  
264 (2002), Evidence in hydrography and density fine structure for enhanced vertical  
265 mixing over the Mid-Atlantic Ridge in the western Atlantic, *J. Geophys. Res.*, 107,  
266 3147, doi:10.1029/2001JC001114.
- 267 Nakano, H. and N. Sugimotohara (2002), Importance of the eastern Indian Ocean for the  
268 abyssal Pacific, *J. Geophys. Res.*, 107, 3219, doi:10.1029/2001JC001065.
- 269 Orsi, A. H., G. C. Johnson, and J. L. Bullister (1999), Circulation, mixing, and  
270 production of Antarctic Bottom Water, *Prog. Oceanogr.*, 43, 55–109.
- 271 Robertson, R., M. Visbeck, A. Gordon, and E. Fahrbach (2002), Long-term temperature  
272 trends in the deep waters of the Weddell Sea, *Deep-Sea Res. II*, 49, 4791–4806.

- 273 Smith, W. H. F. and D. T. Sandwell (1997), Global seafloor topography from satellite  
274 altimetry and ship depth soundings, *Science*, 277, 1957–1962.
- 275 von Storch, H. and F. W. Zwiers (2001), *Statistical Analysis in Climate Research*,  
276 Cambridge University Press, pp. 484.
- 277 Willis, J. K., D. P. Chambers, and R. S. Nerem (2008), Assessing the globally averaged  
278 sea level budget on seasonal to interannual timescales, *J. Geophys. Res.*, 113,  
279 C06015, doi:10.1029/2007JC004517.
- 280 Wright, W. R. (1970), Northward transport of Antarctic Bottom Water in the western  
281 Atlantic Ocean, *Deep-Sea Res.*, 17, 367–371.
- 282 Zenk, W. and E. Morozov (2007), Decadal warming of the coldest Antarctic Bottom  
283 Water flow through the Vema Channel, *Geophys. Res. Lett.*, 34, L14607,  
284 doi:10.1029/2007GJ030340.
- 285



285

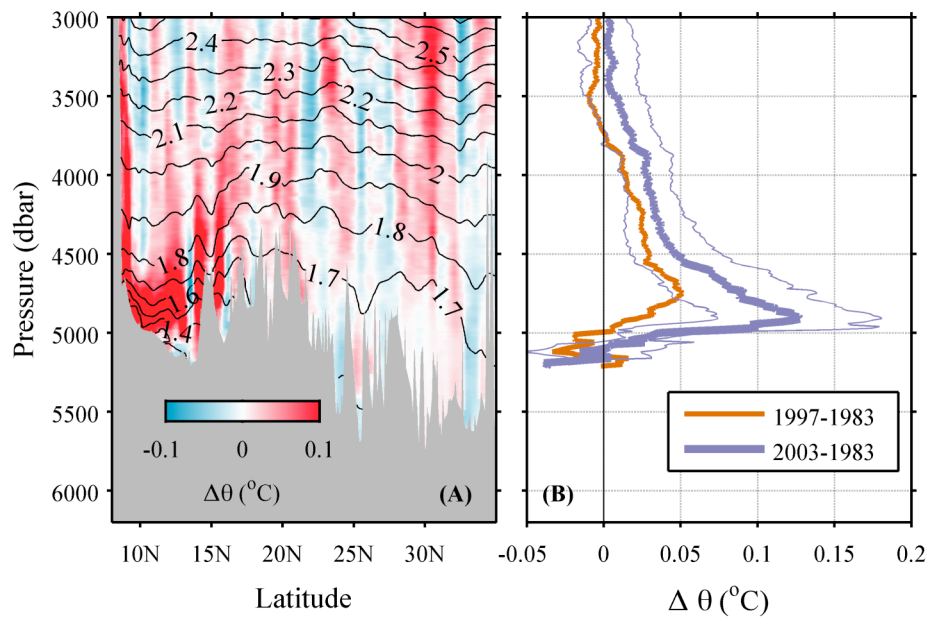
286 **Figure 1.** Station locations from repeat oceanographic sections along 24°N, 52°W, and

287 66°W (see legend) plotted over climatological [Gouretski and Koltermann, 2004]

288 bottom potential temperature, color shaded where  $\theta < 1.8^\circ\text{C}$ . Bathymetry at 1000-m

289 intervals (thin lines) and land (grey shading) are also indicated.

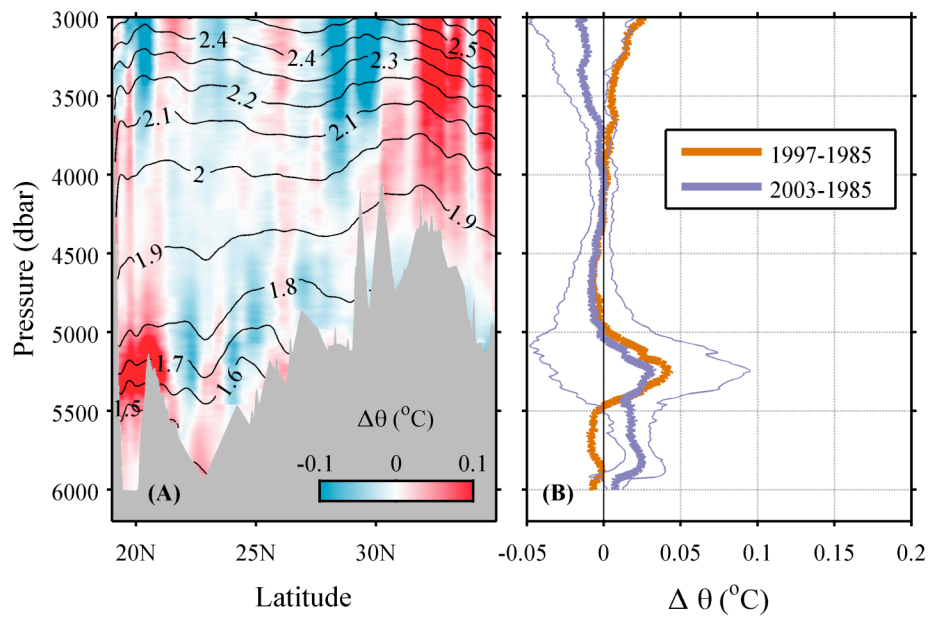
290



290

291 **Figure 2.** Deep  $\theta$  variability along  $52^\circ\text{W}$  (Figure 1). a. Differences in  $\theta$  for 2003 –  
 292 1983 (color shading) south of  $35^\circ\text{N}$  contoured versus pressure and latitude with mean  
 293 potential isotherms (black contours) from 1983, 1997, and 2003 data overlaid and  
 294 bottom bathymetry (grey shading) indicated. b. Mean  $\theta$  differences from  $8 - 18^\circ\text{N}$ , for  
 295 1997 – 1983 (orange line) and 2003 – 1983 (thick blue line) with 95% confidence  
 296 interval (thin blue lines).

297



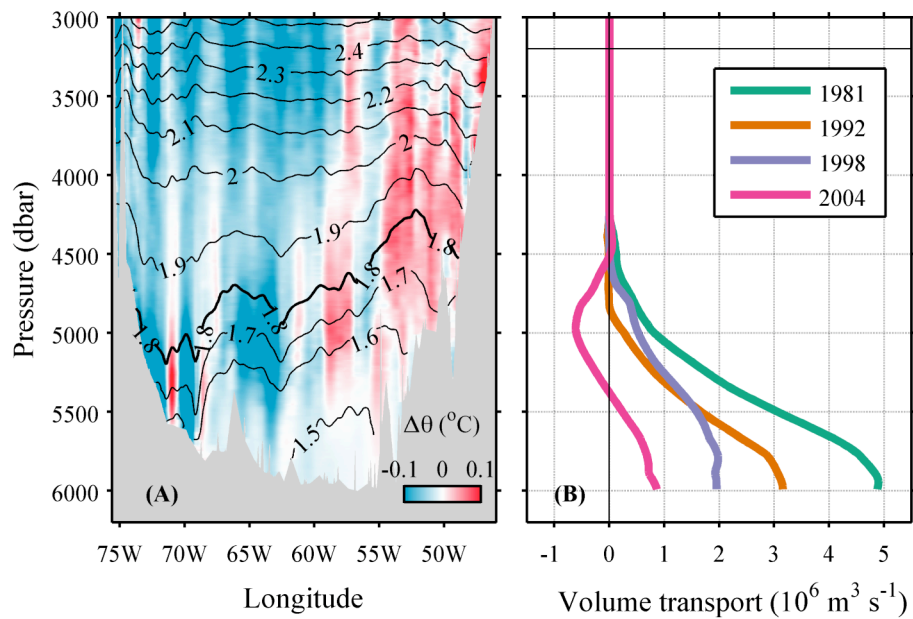
297

298 **Figure 3.** Deep  $\theta$  variability along  $66^\circ\text{W}$  (Figure 1). a. Following Figure 2a but for299 2003 – 1985 along  $66^\circ\text{W}$  from  $18 - 35^\circ\text{N}$  with mean potential isotherms from the 1985,300 1997, and 2005 data. b. Following Figure 2b, but from  $18-27^\circ\text{N}$  along  $66^\circ\text{W}$  for 1997 –

301 1985 and 2003 – 1985.

302





302

303 **Figure 4.** Deep  $\theta$  and volume transport variability across the western basin of the North  
 304 Atlantic at  $24^{\circ}\text{N}$  (Figure 1). a. Deep  $\theta$  differences (color shading) for 2004 – 1981  
 305 contoured versus pressure and longitude with mean potential isotherms (black contours)  
 306 from 1981, 1992, 1998, and 2004 data overlaid and bottom bathymetry (grey shading)  
 307 indicated. b. Cumulative downward vertical integral of meridional geostrophic volume  
 308 transport referenced to a 3200-dbar zero-velocity surface for  $\theta < 1.8^{\circ}\text{C}$  and  $70 - 46^{\circ}\text{W}$   
 309 for 1981, 1992, 1998, and 2004 (see legend).